

The crystal structure and superconducting properties of monatomic bromine

This article has been downloaded from IOPscience. Please scroll down to see the full text article.

2010 J. Phys.: Condens. Matter 22 015702

(<http://iopscience.iop.org/0953-8984/22/1/015702>)

View [the table of contents for this issue](#), or go to the [journal homepage](#) for more

Download details:

IP Address: 129.252.86.83

The article was downloaded on 30/05/2010 at 06:28

Please note that [terms and conditions apply](#).

The crystal structure and superconducting properties of monatomic bromine

Defang Duan¹, Xing Meng¹, Fubo Tian¹, Changbo Chen^{1,2},
Liancheng Wang¹, Yanming Ma¹, Tian Cui^{1,3}, Bingbing Liu¹,
Zhi He¹ and Guangtian Zou¹

¹ State Key Laboratory of Superhard Materials, College of Physics, Jilin University, Changchun 130012, People's Republic of China

² Changchun University of Science and Technology, Changchun 130022, People's Republic of China

E-mail: cuitian@jlu.edu.cn

Received 4 September 2009, in final form 18 October 2009

Published 8 December 2009

Online at stacks.iop.org/JPhysCM/22/015702

Abstract

The crystal structure and superconducting properties of monatomic bromine under high pressure have been studied by first-principles calculations. We have found the following phase transition sequence with increasing pressure: from body-centered orthorhombic (bco, phase II) to body-centered tetragonal structure (bct, phase III) at 126 GPa, then to face-centered cubic structure (fcc, phase IV) at 157 GPa, which is stable at least up to 300 GPa. The calculated superconducting critical temperature $T_c = 1.46$ K at 100 GPa is consistent with the experimental value of 1.5 K. In addition, our results of T_c decrease with increasing pressure in all the monatomic phases of bromine, similar to monatomic iodine. Further calculations show that the decrease of λ with pressure in phase IV is mainly attributed to the weakening of the 'soft' vibrational mode caused by pressure.

(Some figures in this article are in colour only in the electronic version)

1. Introduction

A search for possible high temperature superconductivity in elemental solids under high pressure has attracted considerable interest in recent years. For example, metallic hydrogen is known as one of the ultimate goals for material physicists because it has been predicted to show superconductivity under high pressure with a transition temperature at room temperature [1], even though it has yet to be obtained in the laboratory. However, there has been remarkable progress in the study of other elemental solids at high pressure, such as the light elements lithium and boron [2–4], a surprisingly high T_c of Ca [5], and the group VI elements for oxygen and sulfur [6, 7]. In addition, the superconductivity in the halogen group for iodine and bromine has also been successfully discovered [8–10]. Among various simple elements, iodine and bromine can be regarded as a prototype of hydrogen. Therefore, the studies on the superconductivity of iodine and bromine under high pressure can give us a strong idea in

connection with the possible high- T_c superconductivity in hydrogen.

The consensus has been that the phase transition sequence that happened in both iodine and bromine is from a molecular phase (phase I, space group $Cmca$), to an incommensurate phase (phase V) and then to a monatomic phase (phase II, space group $Immm$) [11–13]. For iodine, the monatomic phase transition sequence is from body-centered orthorhombic (bco, phase II) to body-centered tetragonal structure (bct, phase III) with space group $I4/mmm$ at 43 GPa [14] and then to face-centered cubic structure (fcc, phase IV) with space group $Fm\bar{3}m$, which occurs at 55 GPa [15], and this phase persists to at least 276 GPa [16]. In the case of bromine, the monatomic phase II was estimated as occurring around 115 GPa by the latest high pressure Raman scattering experiment [12], which is higher than that reported in the early experimental investigations [17, 18]. In addition, a first-principles calculation showed that phase V transforms into the monatomic phase II at about 100 GPa [13]. To the best of our knowledge, there has been no further x-ray diffraction

³ Author to whom any correspondence should be addressed.

experimental and theoretical research on the structural phase transitions among the monatomic phases of bromine.

Pressure also causes significant changes in the electronic properties of iodine and bromine. Firstly, an insulator-to-metal transition occurs in the molecular phase before the structure transforms to the monatomic phase [18–21]. Secondly, and more interestingly, the pressure-induced superconductivity [8–10, 22, 23] has been observed in the monatomic metallic phases. In the experimental work of [8], the superconducting critical temperature T_c of iodine decreased with increasing pressure for the bco and bct phases but started to increase with pressure for the fcc phase. The first-principles calculations [22, 23] show that the T_c of both bco and bct under pressures are in agreement with the experimental data, while the T_c of fcc decreases with increasing pressure, contrary to the experimental results. In a recent article, we have explained the conflict between experimental and theoretical results by specifically accounting for non-hydrostatic pressure effects [22]. A similar scheme of pressure-induced phase transformations and superconducting properties can be expected for monatomic bromine, but experimental results are much scarcer than those in the iodine case, which restricts our understanding of the nature of bromine under high pressure. The superconductivity of bromine was observed experimentally between 80 and 120 GPa, giving a T_c of 1.5 K [9]. Up to now, there is no theoretical study on the superconductivity of the monatomic phases in bromine. In this paper, we focus on the high pressure crystal structure and superconducting properties of monatomic bromine by using *ab initio* studies.

The organization of this paper is as follows. In section 2 our computational details are described, in section 3 our results are shown, and the related discussions are given. Finally, in section 4 our results are summarized.

2. Computational details

Calculations of geometrical optimization, vibration properties and the electronic phonon coupling (EPC) parameter were performed using the pseudopotential plane-wave method within the density functional theory (DFT) and linear response theory implemented in the QUANTUM-ESPRESSO package [24]. The geometrical optimizations at 0 K were carried out by using the damped (Beeman) dynamics of the Parrinello–Rahman extended Lagrangian [25], which were not finished until all the stress components were less than 0.05 GPa. Convergence on total energy in the self-consistent field was ensured until 10^{-8} Ryd. For the exchange correlation potential we have used the generalized-gradient approximation (GGA) by Perdew and Wang (PW91) [26], because the GGA provided a much better treatment of solid bromine than the local density approximation (LDA) [13, 27]. The norm-conserving scheme [28] was used to generate the pseudopotential for bromine with an electronic configuration of $4s^2 4p^5$, suitable for the high pressure study. Convergence tests gave a kinetic energy cutoff E_{cutoff} as 70 Ryd and Brillouin zone (BZ) sampling using a grid of spacing $2\pi \times 0.03 \text{ \AA}^{-1}$ in all phases. The EPC calculations were performed on a

$6 \times 6 \times 6$ Monkhorst–Pack (MP) q -point mesh with a denser $24 \times 24 \times 24$ k -point mesh in the bco, and $8 \times 8 \times 8$ MP q -point mesh with a denser $32 \times 32 \times 32$ k -point mesh in the bct and fcc phases for the first BZ integrations. These structures will be described in detail in the text.

The electron–phonon interaction has been investigated by means of Eliashberg theory [29], with the spectral function $\alpha^2 F(\omega)$ obtained by first-principles calculation. The EPC parameter λ is evaluated by a weighted average over the mode EPC parameters λ_{qv} for all phonon modes (qv) in the first BZ:

$$\lambda = \sum_{qv} \lambda_{qv} \omega(q), \quad (1)$$

where $\omega(q)$ is the weight of a sampling q -point in the first BZ. The electron–phonon spectral function $\alpha^2 F(\omega)$ is defined in terms of the phonon linewidth γ_{qv} of mode v at wavevector q as

$$\alpha^2 F(\omega) = \frac{1}{2\pi N(\varepsilon_F)} \sum_{qv} \frac{\gamma_{qv}}{\omega_{qv}} \delta(\omega - \omega_{qv}), \quad (2)$$

where ω_{qv} is the mode frequency and $N(\varepsilon_F)$ is the electronic density of states (DOS) at the Fermi level ε_F . The linewidth of a phonon mode arising from the electron–phonon interaction is given by

$$\gamma_{qv} = 2\pi \omega_{qv} \sum_{kj'} |g_{k+qj',kj}^{qv}|^2 \delta(\varepsilon_{kj} - \varepsilon_F) \delta(\varepsilon_{k+qj'} - \varepsilon_F), \quad (3)$$

where $g_{k+qj',kj}^{qv}$ is the electron–phonon matrix element. The contribution of each vibration mode to the EPC parameter is defined as

$$\lambda_{qv} = \frac{\gamma_{qv}}{\pi \hbar N(\varepsilon_F) \omega_{qv}}. \quad (4)$$

The EPC parameter λ can also be given in terms of the spectral function by

$$\lambda = 2 \int_0^\infty \frac{\alpha^2 F(\omega)}{\omega} d\omega. \quad (5)$$

3. Results and discussion

Figure 1(a) shows a crystal structure of phase II which was found to be a body-centered orthorhombic Bravais lattice (bco, space group $Immm$) with the atoms located on the 2a Wyckoff positions [12, 13]. This phase exhibits a significant anisotropy with the calculated lattice parameters $a = 2.55 \text{ \AA}$, $b = 2.40 \text{ \AA}$ and $c = 4.34 \text{ \AA}$ at 100 GPa. For the special case $a = b$, the bco structure becomes a body-centered tetragonal lattice (bct) which is phase III. If furthermore $c = \sqrt{2}a$, the bct structure becomes the face-centered cubic lattice, which is phase IV. The crystal geometry of the bco structure was optimized for various increasing pressures from 100 to 180 GPa. At each pressure the minimization procedure was reiterated several times since large changes in the unit cell size involved changes of the Brillouin zone grid. The changes of the lattice constants and the ratio b/a and c/a with pressure for monatomic bromine are presented in figures 2(a) and (b), respectively. The lattice vectors reduce anisotropically with increasing external

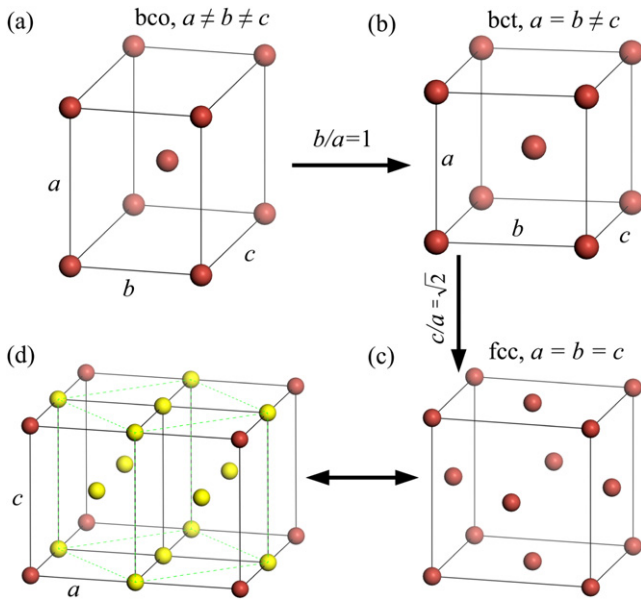


Figure 1. The crystal structures of monatomic bromine for (a) phase II (bco), (b) phase III (bct) and (c) phase IV (fcc). (d) The relation between the bct and fcc unit cell. The fcc unit cell is drawn with green dashed lines.

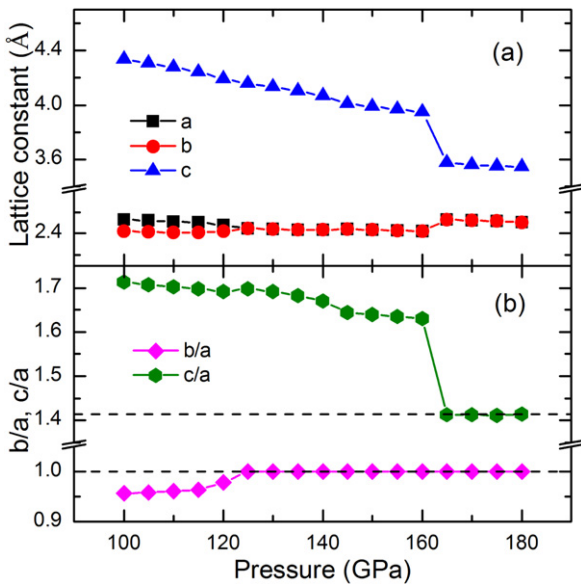


Figure 2. The lattice constants and the ratios b/a and c/a for monatomic bromine under various external pressures.

pressure. The lattice c decreases rapidly with increasing pressure while the lattice a and b reduce appreciably. As can be seen in figure 2, the monotonic decrease of the lattice constants is interrupted and the differences between lattice a and b vanished at about 125 GPa, revealing that phase II transforms into phase III. This phase III is a body-centered tetragonal Bravais lattice with space group $I4/mmm$ and the atoms occupy the 2a Wyckoff positions, as shown in figure 1(b). That is, the atomic coordination becomes isotropic in the tetragonal unique plane while there still exists an anisotropy in the a - c plane. With increasing pressure, the

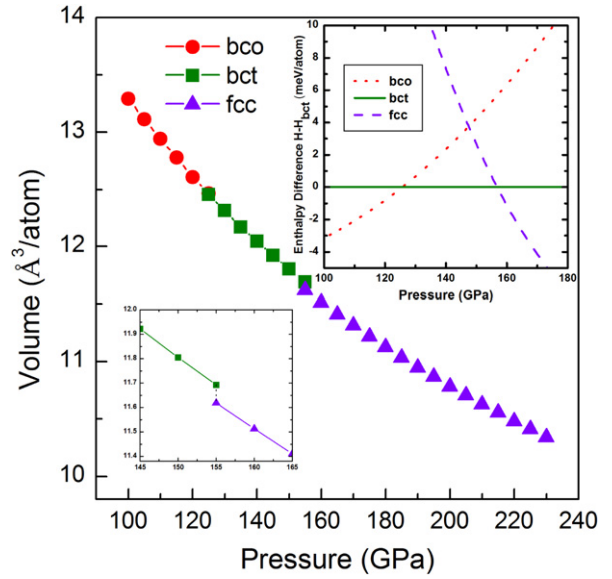


Figure 3. Volume as a function of pressure for three phases of monatomic bromine: bco (red circles), bct (dark cyan squares) and fcc (violet up triangles). Top inset: calculated enthalpy differences (relative to bct structure) as a function of pressure; bco (red dotted line), bct (dark cyan solid line) and fcc (violet dashed line). Bottom inset: the magnified volume–pressure relation around the bct \rightarrow fcc phase transition pressure.

lattice c decreases sharply and the lattice a and b increase abruptly at about 165 GPa. Simultaneously, the ratio c/a exhibits a relatively large decrease: from 1.63 at 160 GPa to $\sqrt{2}$ at 165 GPa, revealing that phase IV is obtained. This phase IV is a face-centered cubic Bravais lattice with space group $Fm\bar{3}m$ and the atoms are located on the 4a Wyckoff positions, as shown in figure 1(c). This structure is isotropic and stable up to the high pressure of 300 GPa, the highest pressure studied. In addition, figure 1(d) shows a schematic representation of the bct and fcc structures: half of the bct structure is a quarter of the fcc structure.

To investigate the phase stability of the crystal structure and to estimate the phase transition pressure, one must evaluate the enthalpy data of all involved phases. The enthalpy differences of the three optimized candidate structures (bco, bct and fcc) as a function of pressure are depicted in the top inset of figure 3. At 100 GPa, the bco structure is the most stable one. When we increase the pressure above 126 GPa, the bco symmetry is broken and the bct phase is favored. Above a pressure of 157 GPa, the enthalpy of the fcc phase is lower than that of the bct phase, suggesting that the fcc structure becomes the most stable one. In addition, the calculated pressure–volume data of monatomic bromine are also plotted in figure 3. The volume change is continuous for the bco to bct transition, supporting a second-order nature, while the volume collapses with 1% for the bct to fcc transition, suggesting the first-order character.

Figure 4 shows the total energy E as a function of lattice a at the selected pressures. It is evident that the $E(a)$ curves exhibit double-well features with two minima located at about $a = 2.42 \text{ \AA}$ and $a = 2.52 \text{ \AA}$, which corresponds to the

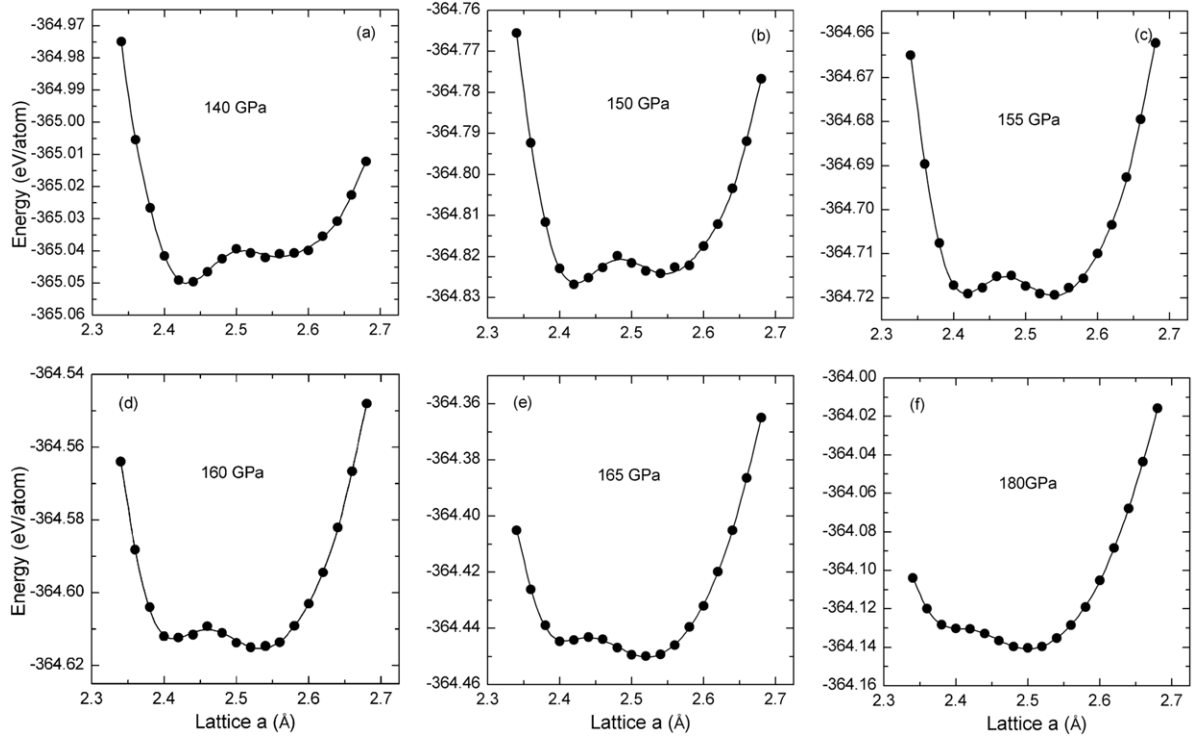


Figure 4. The total energy variations as a function of lattice a for the bct structure at selected pressures.

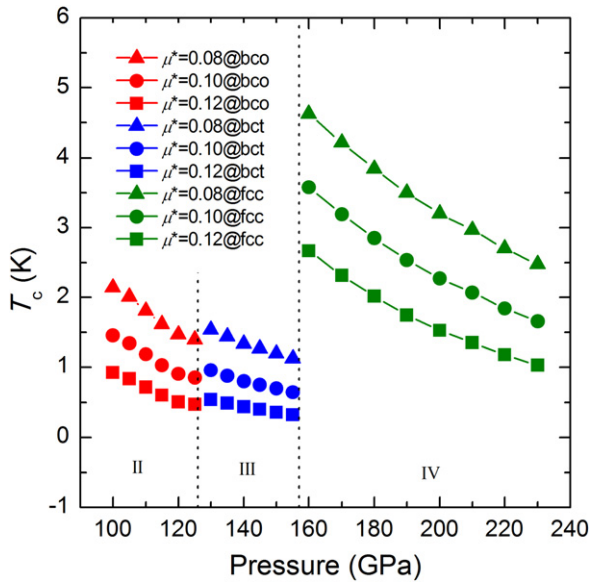


Figure 5. The superconducting critical temperature T_c with several Coulomb potentials μ^* computed at selected pressures. The pressure boundaries between phases II, III and IV are indicated by dotted lines from theoretical results.

bct and fcc structures, respectively. At a low pressure range, the bct structure is found to be more energetically favorable than the fcc structure. With increasing pressure, the local minimum at $a = 2.52 \text{ \AA}$ is gradually lower than the minimum located at $a = 2.42$. As a result, the bct structure is no longer favorable at high pressure, and a transition to the fcc

structure is overwhelmingly preferred. Interestingly, the bct structure transforms to the fcc structure at 157 GPa through comparing the enthalpies (figure 3) or at 165 GPa by structural relaxation (figure 2). From figure 4, we can clearly see that there is a potential barrier between the two local minima, which prevents the structural change observed by structural relaxation at 157 GPa. But with increasing pressure, the potential barrier decreases and the structural change can be observed directly by structural relaxation above 165 GPa.

In this paper, we have successfully mimicked the following phase transition sequence with increasing pressure: from bco (phase II) to bct (phase III) at 126 GPa, then to fcc (phase IV) at 157 GPa. It is similar to the phase transition sequence of monatomic iodine. The sequence of such structural changes (bco–bct–fcc) is a reasonable trend of monatomic bromine to form an isotropic configuration with increasing pressure.

The superconducting critical temperature can be estimated from the Allen–Dynes modified McMillan equation [30] $T_c = \frac{\omega_{\log}}{1.2} \exp\left[-\frac{1.04(1+\lambda)}{\lambda - \mu^*(1+0.62\lambda)}\right]$, where ω_{\log} is the logarithmic average frequency and μ^* is the Coulomb pseudopotential. This equation has been found to be highly accurate for materials with $\lambda < 1.5$. Because of the lack of knowledge of an appropriate value for the Coulomb potential μ^* , there is great difficulty in accurate prediction of T_c . For the weak coupling materials, a standard choice of 0.1 for μ^* is often adopted. However, the value of μ^* for superconductivity in simple elements are quite complex [31–33]. The T_c of monatomic bromine have been calculated with three different values of μ^* from 0.08 to 0.12, as shown in figure 5. At a μ^* of 0.1, a superconducting critical temperature of 1.46 K at 100 GPa

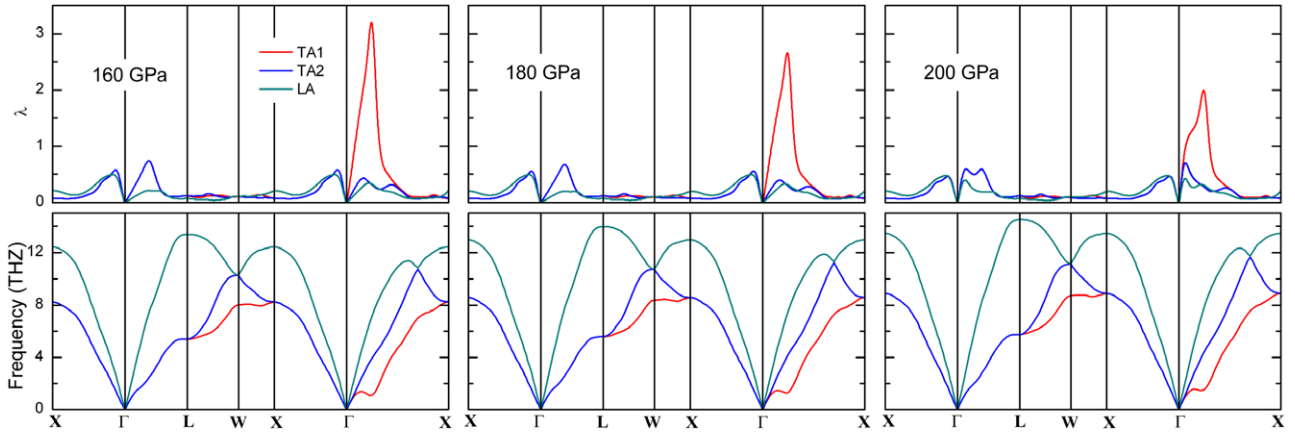


Figure 6. The calculated partial EPC parameters λ and phonon band structure of fcc along the same high-symmetry lines at selected pressures.

Table 1. The electron–phonon coupling parameter λ , logarithmic average of vibrational frequencies ω_{\log} and superconducting critical temperature T_c with $\mu^* = 0.1$ computed in monatomic bromine at selected pressures.

	P (GPa)	ω_{\log} (K)	λ	T_c (K)
bco	100	241.45	0.4280	1.4593
	110	255.19	0.4074	1.1875
	120	272.92	0.3844	0.9060
bct	130	273.78	0.3878	0.9587
	140	285.37	0.3744	0.8033
	150	294.86	0.3645	0.6961
fcc	160	248.41	0.5226	3.5771
	180	268.68	0.4835	2.8491
	200	287.11	0.4525	2.2741

agrees well with the experimental value of 1.5 K [9]. For the bco phase, the superconducting critical temperature T_c decreases with increasing pressure. Similarly to bco, the T_c of the bct phase also decreases with pressure. In the case of the fcc phase, T_c rapidly decreases with increasing pressure. Moreover, T_c jumps to 3.6 K at the transition point, which is nearly five times higher than that of the bct phase. It can be seen that the pressure dependence of T_c in our present work is similar to those theoretical calculations of the monatomic iodine [22].

To probe the origin of the pressure dependence on T_c , we calculate the dynamical properties and EPC parameter λ of the three structures mentioned in this paper. Assuming μ^* is a constant, two parameters, the EPC parameter λ and the logarithmic average frequency ω_{\log} , determine T_c . Values of these parameters computed at selected pressures are summarized in table 1. For the bco, bct, and fcc, ω_{\log} increases with increasing pressure, while λ decreases, but the changing rate of λ exceeds that of ω_{\log} . As a result, the value of T_c decreases with pressure mainly due to the decrease of λ .

The phonon band structure of fcc at different pressures is shown in figure 6. The absence of imaginary frequency modes indicates that the structure is stable in the pressure range. A striking feature of the phonon band structure is the presence of a ‘softening’ in the lowest transverse acoustic

(TA1) mode along the Γ –K $[\xi\xi0]$ direction. To explore the dependence of the EPC on soft phonon modes, the partial EPC parameter λ for the three branches along several high-symmetry directions is also depicted in figure 6. It can be clearly seen that the ‘softening’ exists in the lowest transverse acoustic (TA1) mode along the Γ –K $[\xi\xi0]$ direction, leading to a significant electron–phonon contribution, in which a high and broad peak of λ for the fcc structure is observed near the q -point. As pressure increases, soft vibrational modes gradually fade away, resulting in the intensity of the main peak of λ decreasing correspondingly, as shown in figure 6. Therefore, the decrease of λ of the fcc phase under compression mainly derives from the fade away of soft vibrational modes induced by increasing pressure.

The partial EPC constant λ and phonon spectrum of the bco and bct are shown in figure 7. The absence of imaginary frequency modes indicates that both structures are stable. For the bco and bct structure, there is no obvious soft phonon mode observed and the value of the main peaks of λ is small. But the intensity of the main peaks are clearly seen as a decrease with increasing pressure (not shown).

From table 1, we find that T_c in the fcc phase is more than five times as large as in the bct phase in the bct \rightarrow fcc phase transition domain. Even though the ω_{\log} of the fcc phase is smaller than that of the bct phase, the EPC parameter λ in the fcc phase was found to be 1.5 times bigger than that of the bct phase. This comes from the soft phonon mode along the $[\xi\xi0]$ direction in the fcc phase. Therefore, this sharp increase of the T_c is attributed to the bigger λ due to the softening of the phonon observed in our first-principles calculation.

4. Conclusions

In summary, we have presented a first-principles investigation of the crystal structure and superconducting properties of monatomic bromine. The transition from the bco (phase II) to bct (phase III) occurs at 126 GPa, then the bct transforms to the fcc (phase IV) at 157 GPa, and the bct to fcc structural transition further verified by the total energy calculation. It is found that the fcc phase is stable at least up to 300 GPa,

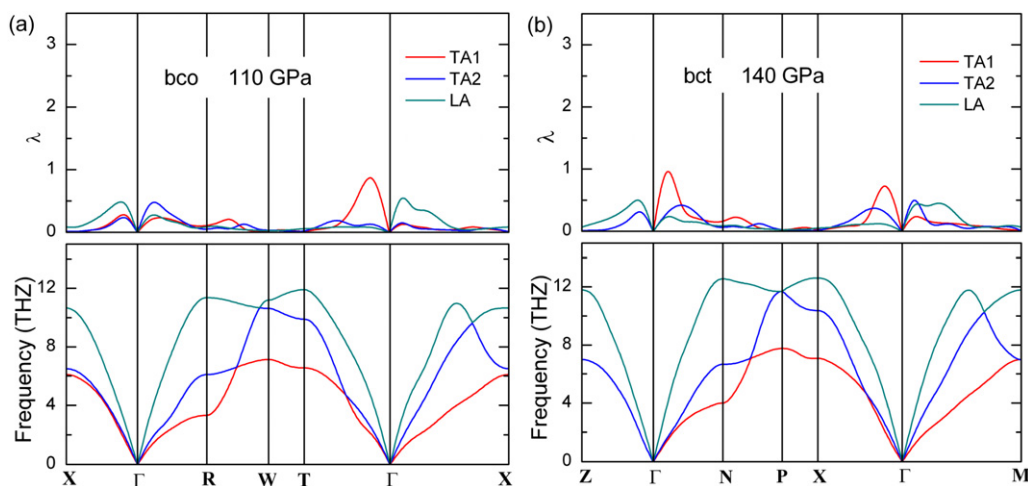


Figure 7. The calculated partial EPC parameters λ and phonon band structure of bco and bct along same high-symmetry lines at 110 and 140 GPa in (a) and (b), respectively.

the highest pressure studied. The calculated superconducting critical temperature T_c is in agreement with the experimental results [9]. Moreover, the calculated T_c decreases with pressure in phase II, phase III and phase IV, similar to monatomic iodine. Further EPC calculations reveal that the decrease of λ of the fcc phase under pressure mainly derives from the fade away of soft vibrational modes induced by increasing pressure.

Acknowledgments

This work was supported by the National Natural Science Foundation of China (nos. 10574053 and 10674053), the National Basic Research Program of China (no. 2005CB724400), the 2007 Cheung Kong Scholars Program of China, Changjiang Scholar and Innovative Research Team in University (no. IRT0625) and the National Found for Fostering Talents of Basic Science (no. J0730311).

References

- [1] Richardson C F and Ashcroft N W 1997 *Phys. Rev. Lett.* **78** 118
- [2] Shimizu K, Ishikawa H, Takao D, Yagi T and Amaya K 2002 *Nature* **419** 597
- [3] Deemyad S and Schilling J S 2003 *Phys. Rev. Lett.* **91** 167001
- [4] Eremets M I, Struzhkin V V, Mao H K and Hemley R J 2001 *Science* **293** 272
- [5] Yabuuchi T, Matsuoka T, Nakamoto Y and Shimizu K 2006 *J. Phys. Soc. Japan* **75** 083703
- [6] Shimizu K, Suhara K, Ikumo M, Eremets M I and Amaya K 1998 *Nature* **393** 767
- [7] Struzhkin V V, Hemley R J, Mao H K and Timofeev Y A 1997 *Nature* **390** 382
- [8] Shimizu K, Yamauchi T, Tamitani N, Takeshita N, Ishizuka M, Amaya K and Endo S 1994 *J. Supercond.* **7** 921
- [9] Shimizu K, Amaya K and Endo S 1995 *Rev. High Pressure Sci. Technol.* **4** 498
- [10] Amaya K, Shimizu K, Eremets M I, Kobayashi T C and Endo S 1998 *J. Phys.: Condens. Matter* **10** 11179
- [11] Kenichi T, Kyoko S, Hiroshi F and Mitsuko O 2003 *Nature* **423** 971
- [12] Kume T, Hiraoka T, Ohya Y, Sasaki S and Shimizu H 2005 *Phys. Rev. Lett.* **94** 065506
- [13] Duan D, Liu Y, Ma Y, Liu Z, Cui T, Liu B and Zou G 2007 *Phys. Rev. B* **76** 104113
- [14] Fujii Y, Hase K, Ohishi Y, Hamaya N and Onodera A 1986 *Solid State Commun.* **59** 85
- [15] Fujii Y, Hase K, Hamaya N, Ohishi Y, Onodera A, Shimomura O and Takemura K 1987 *Phys. Rev. Lett.* **58** 796
- [16] Reichlin R, McMahan A K, Ross M, Martin S, Hu J, Hemley R J, Mao H K and Wu Y 1994 *Phys. Rev. B* **49** 3725
- [17] Fujii Y, Hase K, Ohishi Y, Fujihisa H, Hamaya N, Takemura K, Shimomura O, Kikegawa T, Amemiya Y and Matsushita T 1989 *Phys. Rev. Lett.* **63** 536
- [18] Fujihisa H, Fujii Y, Takemura K and Shimomura O 1995 *J. Phys. Chem. Solids* **56** 1439
- [19] Riggelman B M and Drickamer H G 1963 *J. Chem. Phys.* **38** 2721
- [20] Miyagi H, Yamaguchi K, Matsuo H and Mukose K 1998 *J. Phys.: Condens. Matter* **10** 11203
- [21] Mukose K, Fukano R, Miyagi H and Yamaguchi K 2002 *J. Phys.: Condens. Matter* **14** 10441
- [22] Duan D, Jin X, Ma Y, Cui T, Liu B and Zou G 2009 *Phys. Rev. B* **79** 064518
- [23] Sakamoto H, Oda T, Shirai M and Suzuki N 1996 *J. Phys. Soc. Japan* **65** 489
- [24] Baroni S, Dal Corso A, de Gironcoli S, Giannozzi P, Cavazzoni C, Ballabio G, Scandolo S, Chiarotti G, Focher P, Pasquarello A, Laasonen K, Trave A, Car R, Marzari N and Kokalj A <http://www.pwscf.org/>
- [25] Parrinello M and Rahman A 1980 *Phys. Rev. Lett.* **45** 1196
- [26] Parrinello M and Rahman A 1981 *J. Appl. Phys.* **52** 7182
- [27] Perdew J P, Chevary J A, Vosko S H, Jackson K A, Pederson M R, Singh D J and Fiolhais C 1992 *Phys. Rev. B* **46** 6671
- [28] Miao M S, Van Doren V E and Martins J L 2003 *Phys. Rev. B* **68** 094106
- [29] Troullier N and Martins J L 1991 *Phys. Rev. B* **43** 1993
- [30] Eliashberg G M 1960 *Zh. Eksp. Teor. Fiz.* **38** 966
- [31] Eliashberg G M 1960 *Sov. Phys.—JETP* **11** 696 (Engl. Transl.)
- [32] Allen P B and Dynes R C 1975 *Phys. Rev. B* **12** 905
- [33] Richardson C F and Ashcroft N W 1997 *Phys. Rev. B* **55** 15130
- [34] Ma Y, Tse J S, Cui T, Klug D D, Zhang L, Xie Y, Niu Y and Zou G 2005 *Phys. Rev. B* **72** 014306
- [35] Yao Y and Tse J S 2007 *Phys. Rev. B* **75** 134104